Study of the production of Z boson pairs in e^+e^- collisions at LEP with the L3 detector

S. Hou for the L3 collaboration
National Central University, Taiwan

At the center-of-mass energy of 183 GeV attained by the LEP e^+e^- collider in 1997, the threshold production of a Z pair has become accessible. This phenomenon is enhanced for the higher cross section and integrated luminosity of the 1998 run at 189 GeV. We report on the study of all the visible decay modes of this pair. Combining all these final states the presence of a non vanishing signal is established at more than 95% of confidence level at 183 GeV and its cross section is measured to be in agreement with the Standard Model predictions. No evidence for the existence of anomalous triple gauge boson ZZZ and ZZγ couplings is found and limits on their value are set. Preliminary results at 189 GeV are also discussed.

I. INTRODUCTION

The production of on-shell Z boson pairs has become accessible at LEP in 1997 and 1998 with the center-of-mass energy at and above the ZZ threshold. In this note we present the L3 measurement of the Z pair production and the interpretation with anomalous ZZZ and ZZγ coupling in all the visible decay modes of $\ell^+\ell^-\mathrm{q\bar{q}}$, $\ell^+\ell^-\ell'^+\ell'^-$, $\ell^+\ell^-\nu\bar{\nu}$, $\mathrm{q\bar{q}}\nu\bar{\nu}$ and $\mathrm{q\bar{q}q'\bar{q}'}$ [1,2]. The data analyzed correspond to an integrated luminosity of 55.3 pb^{-1} and 176.4 pb^{-1} at center-of-mass energy of 182.72 and 188.66 GeV, respectively, denoted hereafter as 183 and 189 GeV.

II. SELECTION OF ON-SHELL ZZ EVENTS

The process $e^+e^- \rightarrow$ ZZ is described by the conversion diagram in the Standard Model via the t-channel exchange of an electron. The EXCALIBUR [3] Monte Carlo is used to simulate the neutral-current four-fermion events. The on-shell ZZ signal is defined by phase-space cuts at generator level requiring the masses of the generated fermion pairs in the final state to be in the range between 70 GeV and 105 GeV. If the four fermions are of the same flavor, for at least one of the two possible fermion pair combinations, the fermion pair masses must be in the range mentioned above. There is a large contribution from W exchange in the final states $\mathrm{u\bar{u}d\bar{d}}$, $\mathrm{c\bar{c}s\bar{s}}$ and $\nu_\ell\bar{\nu}_\ell\ell^+\ell^-$ ($\ell = \mathrm{e}, \mu, \tau$). To reduce this contribution we require that the masses of the fermion pairs susceptible to come from a W decay be either smaller than 75 GeV or larger than 85 GeV. The total expected ZZ cross section within these cuts is 0.25 pb at 183 GeV, and 0.62 pb at 189 GeV. Contributions from different final states are reported in Table I.

A. The ZZ $\rightarrow\ell^+\ell^-\mathrm{q\bar{q}}$ channel

The ZZ$\rightarrow$ $\ell^+\ell^-\mathrm{q\bar{q}}$ selections are performed for final states with electrons, muons and taus. Hadronic events containing leptons are selected with thresholds applied on the visible energy and lepton energy. The opening angle between the two electrons or muons and the two jets has to exceed 120°. The $e^+e^-\mathrm{q\bar{q}}$ and $\mu^+\mu^-\mathrm{q\bar{q}}$ events are subject to the DURHAM algorithm requiring $\log(\mathrm{Y}_{34}) \geq -6$, with Y_{34} the parameter separating an event from a four-jet to a three-jet topology. For the $e^+e^-\mathrm{q\bar{q}}$ channel we require in addition the invariant mass of the two electrons to be larger than 70 GeV and the ratio of the missing transverse momentum to the visible energy to be less than 0.1.

TABLE I. Cross sections calculated with EXCALIBUR for the ZZ signal.

ZZ $\rightarrow$	$\mathrm{q\bar{q}q'\bar{q}'}$	$\mathrm{q\bar{q}}\nu\bar{\nu}$	$\ell^+\ell^-\mathrm{q\bar{q}}$	$\ell^+\ell^-\nu\bar{\nu}$	$\ell^+\ell^-\ell'^+\ell'^-$	$\nu\bar{\nu}\nu'\bar{\nu}'$	Sum
$\sigma(\sqrt{s}$=182.72 GeV) (fb)	116	63.0	43.4	12.0	6.5	8.8	250
$\sigma(\sqrt{s}$=188.66 GeV) (fb)	290	170	97.4	27.1	11.2	24.8	620

The $\tau^+\tau^-\mathrm{q\bar{q}}$ events are selected by a tau identification and a jet based algorithms. In the first algorithm, tau leptons are identified via their decay into isolated electrons or muons, or as an isolated low-multiplicity jet with 1 or 3 tracks and unit charge. In the jet based algorithm, the event is forced into four jets using the DURHAM algorithm. Two of the jets must have less than 4 tracks. These jets are then considered as τ candidates. An event is accepted if it satisfies either of the two selections. The opening angle between the two τ candidates and between the two jets must be larger than 130°. Their invariant masses must be within 70 GeV and 120 GeV.

The results for the $\ell^+\ell^-\mathrm{q\bar{q}}$ event selections at 183 and 189 GeV are summarized in Table II and III, respectively. The spectra of the mass obtained from a kinematic fit, imposing four-momentum conservation and equal masses of the lepton and the jet pair, $\mathrm{M_{5C}}$, are shown in Fig. 1.a and 2.a for data and Monte Carlo samples at 183 and 189 GeV, respectively. The background is dominated by $\mathrm{W^+W^-} \rightarrow \ell\nu\mathrm{q\bar{q}}$ events. The remaining background consists of $\mathrm{e^+e^-} \rightarrow \mathrm{q\bar{q}}(\gamma)$ and neutral-current four-fermion events outside the ZZ signal definition cuts. The errors on signal and background predictions are dominated by uncertainties in the energy scale, the lepton identification and isolation. An error of 15% on the expected number of background events and 4% on the signal efficiency is assigned.

B. The ZZ $\rightarrow\ell^+\ell^-\ell'^+\ell'^-, \ell^+\ell^-\nu\bar{\nu}$ channels

The ZZ$\rightarrow$ $\ell^+\ell^-\ell'^+\ell'^-$ selection is developed for all charged leptonic final states other than $\tau^+\tau^-\tau^+\tau^-$ events. At least four leptons are required in the event. The electrons must have an energy of at least 15 GeV, relaxed to 3 GeV for other leptons. The invariant masses of the combinations of two same flavor leptons are then calculated and the lepton pair whose mass is the closest to the Z boson mass is chosen. This mass ($\mathrm{M_{ll}}$) and the recoil mass ($\mathrm{M_{rec}}$) to the chosen lepton pair are required to be in the range between 70 GeV and 105 GeV. The distribution of the average of these two masses ($\mathrm{M_{av}}$) is shown in Fig. 1.b for 183 GeV data, and their sum in Fig. 2.b for 189 GeV data.

The $\ell^+\ell^-\nu\bar{\nu}$ events, with ℓ either a muon or an electron, are selected requiring two same flavor leptons. These event are required to have less than 3 tracks, less than 6 calorimetric clusters and a visible energy in the range between 80 GeV and 100 GeV. The lepton pair mass ($\mathrm{M_{vis}}$) must be in the range 70 GeV to 105 GeV and the mass recoiling against the leptons ($\mathrm{M_{rec}}$) in the range 70 GeV to 100 GeV. Their sum are shown in Fig. 1.c and 2.c for 183 and 189 GeV data, respectively.

The main background to these channels are constituted by lepton pair production and neutral and charged-current four-fermion events outside the ZZ signal definition cuts. The errors on the expected signal and background events are due to the lepton identification and the limited Monte Carlo statistics. The signal efficiency depends on the final state. The signal efficiency, the expected signal and background and the observed events at 183 and 189 GeV are reported in Table II and III, respectively. Errors of 25% and 10% are assigned to the expected number of background and signal events, respectively, for $\ell^+\ell^-\ell'^+\ell'^-$, and 10% for both signal and background for the $\ell^+\ell^-\nu\bar{\nu}$ final state.

C. The ZZ $\rightarrow\mathrm{q\bar{q}}\nu\bar{\nu}$ channel

The ZZ$\rightarrow$ $\mathrm{q\bar{q}}\nu\bar{\nu}$ events are selected for high multiplicity hadronic events with energy deposition in the electromagnetic calorimeter larger than 10 GeV. The event is forced to form two jets using the DURHAM algorithm. The invariant mass of the two jets, $\mathrm{M_{vis}}$, must be in the range 60 GeV to 125 GeV. The multiperipheral $\mathrm{e^+e^-} \rightarrow \mathrm{e^+e^-f\bar{f}}$ events are suppressed by requiring the energy in the low polar angle calorimeters to be smaller than 10 GeV. The $\mathrm{e^+e^-} \rightarrow \mathrm{q\bar{q}}(\gamma)$ events are rejected requiring the transverse missing energy larger than 5 GeV and the longitudinal momentum less than 40% of the visible energy. To reduce the remaining background from $\mathrm{e^+e^-} \rightarrow \mathrm{W^+W^-}$ production, events containing identified leptons with energy greater than 20 GeV are rejected.

To further differentiate between the signal and the $\mathrm{W^+W^-}$ background, the discriminant variable NN is constructed using a neural network approach. The inputs to the neural network include event shape variables, the event mass, the masses of the two jets and the total missing momentum. The signal events populate preferentially the region of high NN values. A lower cut on the NN variable is applied to maximize the signal to background ratio.

TABLE II. Signal efficiencies, expected number of signal and background events and data for all ZZ final states at 183 GeV.

Process ZZ →	Signal efficiency (%)	Signal events	Background events	Data events
$e^+e^-q\bar{q}$	79	0.79 ± 0.03	0.29 ± 0.04	2
$\mu^+\mu^-q\bar{q}$	58	0.42 ± 0.02	0.09 ± 0.01	0
$\tau^+\tau^-q\bar{q}$	36	0.26 ± 0.01	0.85 ± 0.13	0
$\ell^+\ell^-\ell'^+\ell'^-$	15-78	0.13 ± 0.01	0.12 ± 0.03	0
$\ell^+\ell^-\nu\bar{\nu}$	37^a, 33^b	0.18 ± 0.02	1.23 ± 0.12	2
$q\bar{q}\nu\bar{\nu}$	47	1.64 ± 0.07	13.0 ± 0.7	12
$q\bar{q}q'\bar{q}'$	34	2.26 ± 0.14	46 ± 2	47

TABLE III. Preliminary results of signal efficiencies, expected number of signal and background events and data at 189 GeV.

Process ZZ →	Signal efficiency (%)	Signal events	Background events	Data events
$\ell^+\ell^-q\bar{q}$	$73^c, 55^d, 28^e$	10	5	14
$\ell^+\ell^-\ell'^+\ell'^-$	28-66	0.7	0.6	2
$\ell^+\ell^-\nu\bar{\nu}$	$29^a, 21^b$	0.7	1.2	3
$q\bar{q}\nu\bar{\nu}$	61	19	39	61
$q\bar{q}q'\bar{q}'$	58	32	663	714

$^a(e^+e^-\nu\bar{\nu})$, $^b(\mu^+\mu^-\nu\bar{\nu})$ $^c(e^+e^-q\bar{q})$, $^d(\mu^+\mu^-q\bar{q})$, $^e(\tau^+\tau^-q\bar{q})$

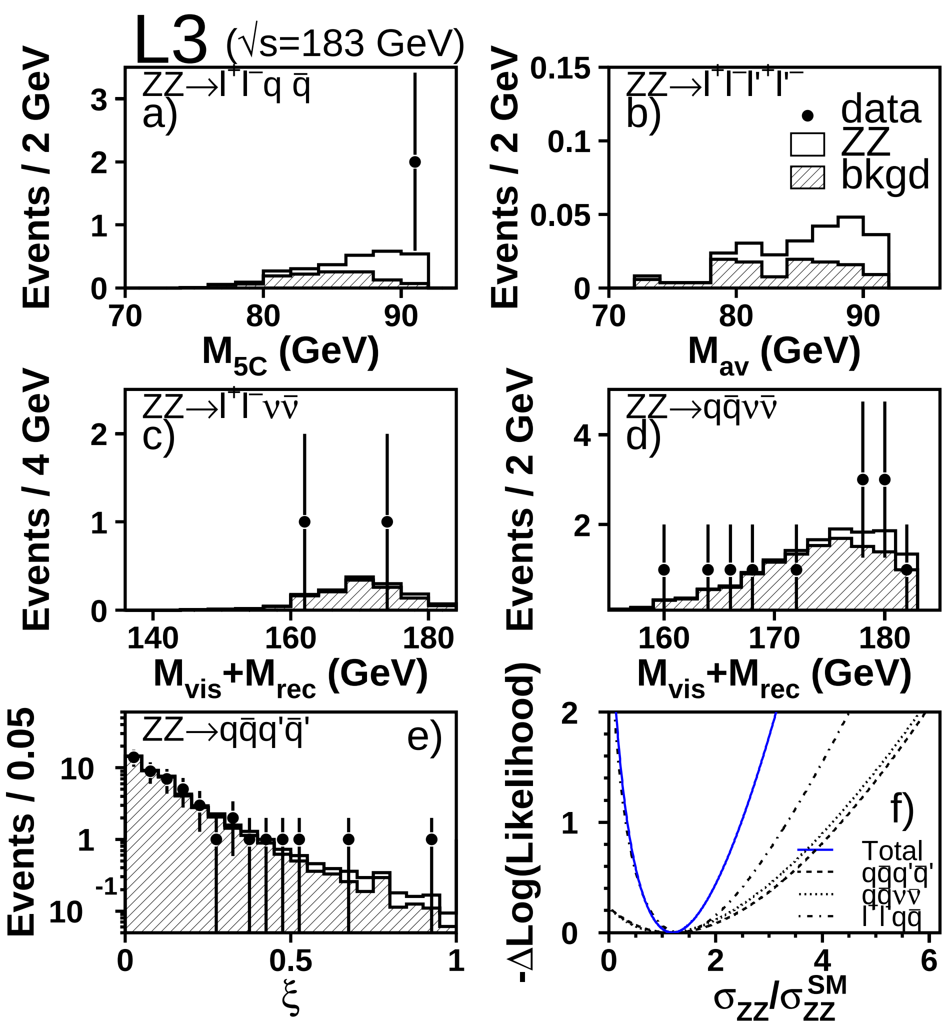

FIG. 1. Distributions of selected ZZ events at 183 GeV in the decay channels : a) $\ell^+\ell^-q\bar{q}$, b) $\ell^+\ell^-\ell'^+\ell'^-$, c) $\ell^+\ell^-\nu\bar{\nu}$, d) $q\bar{q}\nu\bar{\nu}$, e) $q\bar{q}q'\bar{q}'$, and f) the likelihoods as a function of the ratio of measured and the Standard Model prediction.

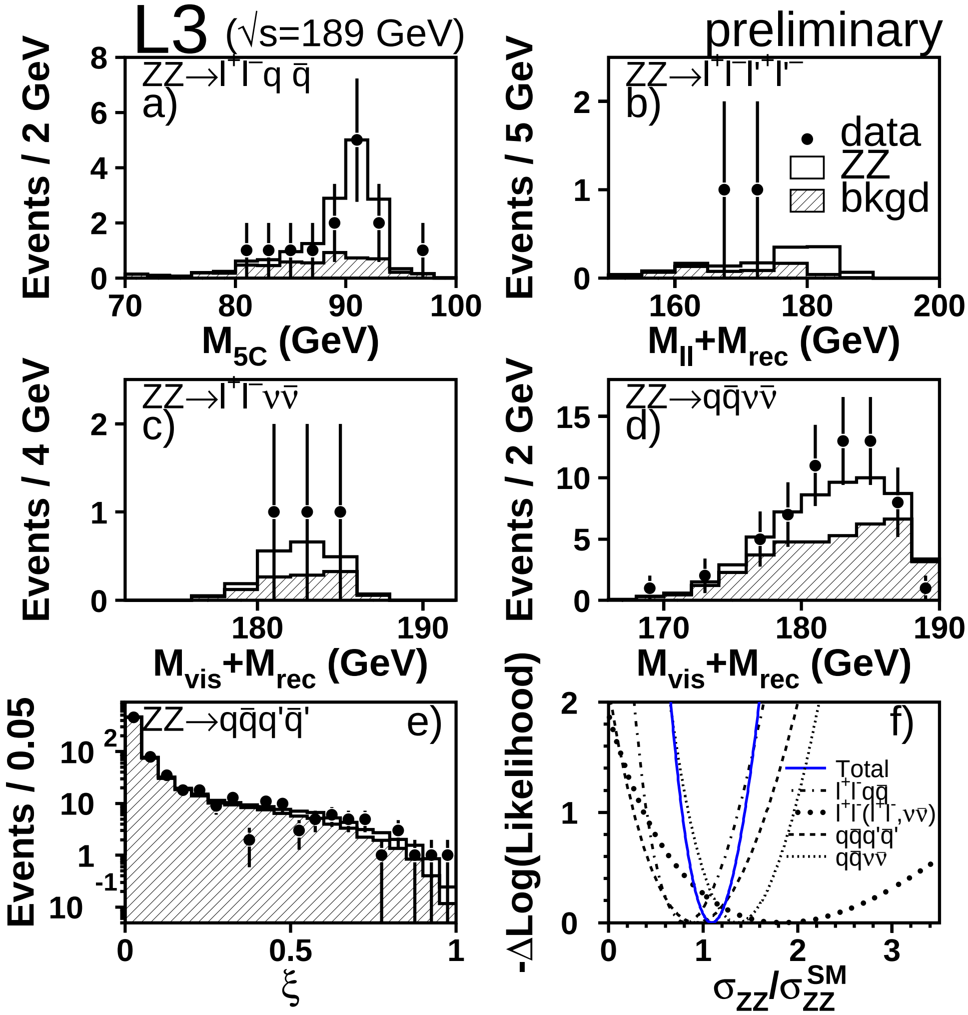

FIG. 2. Distributions of selected ZZ events at 189 GeV in the decay channels : a) $\ell^+\ell^-\mathrm{q\bar{q}}$, b) $\ell^+\ell^-\ell'^+\ell'^-$, c) $\ell^+\ell^-\nu\bar{\nu}$, d) $\mathrm{q\bar{q}}\nu\bar{\nu}$, e) $\mathrm{q\bar{q}q'\bar{q}'}$, and f) the likelihoods as a function of the ratio of measured and the Standard Model prediction.

The sum of visible and recoil masses ($\mathrm{M_{vis}} + \mathrm{M_{rec}}$) is shown in Fig. 1.d and 2.d, for 183 and 189 GeV data, respectively, and the corresponding signal efficiency, the expected signal and background and the observed events are reported in Table II and III, respectively. The errors on signal and background expectations are mainly determined by the uncertainty on the energy calibration and the limited Monte Carlo statistics: they are 4% and 5% for signal and background, respectively.

D. The ZZ $\rightarrow\mathrm{q\bar{q}q'\bar{q}'}$ channel

The ZZ$\rightarrow$ $\mathrm{q\bar{q}q'\bar{q}'}$ events are selected for high multiplicity hadronic events with visible energy close to the center-of-mass energy. The four jets are reconstructed using the Durham algorithm and fit with the four-momentum conservation imposed to improve the di-jet mass resolution. The four jets are paired into two di-jets, each of which is required to have more than four tracks, to suppress the contamination from $\tau^+\tau^-\mathrm{q\bar{q}}$ events. Of the three possible pairing combinations, the one with minimum mass χ^2 to the assumption of a Z pair is chosen.

A neural network method is used to distinguish the ZZ $\rightarrow\mathrm{q\bar{q}q'\bar{q}'}$ events from the $\mathrm{e^+e^-}\rightarrow\mathrm{q\bar{q}}(\gamma)$ and $\mathrm{e^+e^-}\rightarrow\mathrm{W^+W^-}$ backgrounds. The input variables are chosen for the event topological variables, kinematic variables of jets, ratio of energies and opening angles of the jets, and the χ^2 values of equal mass fits for W^+W^- or ZZ pairs hypotheses. The discriminant variable, $\xi = NN_{ZZ}(1 - NN_{qq})(1 - NN_{WW})(2M_{5C}/\sqrt{s})$, is a convolution of the three neural network outputs for $e^+e^- \rightarrow q\bar{q}(\gamma)$, W^+W^- and ZZ events, denoted as NN_{qq}, NN_{WW} and NN_{ZZ}, respectively, and the invariant mass M_{5C} obtained from a kinematic fit imposing four-momentum conservation and equal mass for the two di-jets.

The signal events populate in the region of high ξ values. To improve the signal to background ratio, a cut of $M_{5C} > 85$ GeV is imposed for data of 183 GeV and the ξ distribution is shown in Fig. 1.e. This cut is relaxed for 189 GeV data and the ξ distribution is shown in Fig. 2.e. The signal efficiency, expected signal, background and observed data events are reported in Table II and III for 183 and 189 GeV data, respectively. The errors on signal and background expectations are mainly determined by the uncertainty on the energy calibration and the limited Monte Carlo statistics: they are 6% and 4% for signal and background, respectively.

III. MEASUREMENT OF THE ZZ CROSS SECTION

The spectra of all decay channels are used in a binned Poissonian log-likelihood fit for the ratio of the measured cross section to the Standard Model value as predicted by EXCALIBUR. The likelihoods of the most significant channels and the combined one are illustrated in Fig. 1.f and Fig. 2.f, for 183 and 189 GeV, respectively. The measured cross sections are

$$\sigma_{ZZ} = 0.30^{+0.22\,+0.07}_{-0.16\,-0.03}\ \text{pb} \quad (\sigma_{ZZ}^{SM} = 0.25\ \text{pb}), \quad \text{at 183 GeV;}$$
$$\sigma_{ZZ} = 0.68^{+0.15}_{-0.14}\ \text{pb} \quad (\sigma_{ZZ}^{SM} = 0.62\ \text{pb}), \quad \text{at 189 GeV, preliminary.}$$

At 183 GeV the systematic error is estimated taking into account the errors on signal and background expectations reported in Table II, and $0.03 < \sigma_{ZZ} < 0.79$ pb is obtained at 95 % confidence level. The error at 189 GeV is statistical only. The measured cross section values are in good agreement with the Standard Model.

IV. LIMITS ON ANOMALOUS COUPLINGS

The most general Lorentz invariant expressions including anomalous couplings are given in Ref. [4]. Deviations from the Standard Model are described by means of four anomalous couplings f_i^V $(i = 4, 5; V = \gamma, Z)$, where the V superscript corresponds to an anomalous coupling ZZV. The anomalous couplings f_5^V lead to violation of C and P symmetries while f_4^V introduces CP violation. At tree level these couplings are zero in the Standard Model.

In order to calculate the impact of anomalous couplings on the measured distributions in the process $e^+e^- \rightarrow f\bar{f}f'\bar{f}'$, the EXCALIBUR generator is extended to have all matrix elements of conversion diagrams with two Z bosons supplemented by an additional term containing anomalous couplings. Using the distributions given in Fig. 1.a-e and 2.a-e, a binned maximum likelihood fit is performed for each of the anomalous couplings f_i^V fixing the others to zero. The results for all couplings are consistent with the Standard Model values of zero and 95% confidence level limits on the parameters f_i^V are set

$$-3.6 \le f_4^Z \le 3.4 \quad -8.4 \le f_5^Z \le 7.9 \quad -2.1 \le f_4^\gamma \le 2.1 \quad -4.9 \le f_5^\gamma \le 4.8 \qquad \text{at 183 GeV;}$$
$$-1.7 \le f_4^Z \le 1.8 \quad -4.7 \le f_5^Z \le 4.7 \quad -1.0 \le f_4^\gamma \le 1.1 \quad -2.8 \le f_5^\gamma \le 2.9 \qquad \text{at 189 GeV, preliminary.}$$

[1] L3 Collab., M. Acciarri *et al.*, CERN-EP/98-206, December 17, 1998; to be published in Phys. Lett. **B**.
[2] J. Alcaraz *et al.*, "Preliminary Results on Neutral Gauge Boson Production in e^+e^- interactions at $\sqrt{s} = 189$ GeV", L3 Note 2366, March 5, 1999.
[3] F.A. Berends, R. Kleiss and R. Pittau, Nucl. Phys. **B 424** (1994) 308; Nucl. Phys. **B 426** (1994) 344; Nucl. Phys. (Proc. Suppl.) **B 37** (1994) 163; Phys. Lett. **B 335** (1994) 490; R. Kleiss and Pittau, Comp. Phys. Comm. **83** (1994) 14.
[4] K. Hagiwara *et al.*, Nucl. Phys. **B 282** (1987) 253.